Schwartz-Christoffel Transformation applied to Polygons and Airfoils

Etsuo Morishita

Abstract—Potential flows around polygons and airfoils are obtained by the Schwartz-Christoffel transformation. Although the Schwartz-Christoffel transformation is well known, the application to the flow problems is limited to relatively simple flows. The present author extended the method to flows around regular and other simple polygons. This is possible by mapping a circle to a polygon. It is reminded that a flat plate from the Joukowsky transformation is also included in the Schwartz-Christoffel one. It is interesting to note that the Schwartz-Christoffel transformation can be applicable to a two-dimensional airfoil approximated as a polygon.

Keywords—Aerodynamics, Airfoil, Conformal mapping, Potential flow,.

I. INTRODUCTION

Schwartz-Christoffel transformation is introduced in text books of fluid dynamics [1]. However, its applications are limited to relatively simple flow fields. The Schwartz-Christoffel transformation was applied to a flow around a flat-plate rudder [2]. Present author extended the transformation to two-dimensional airfoils. A two-dimensional airfoil can be approximated as a polygon like panel methods [3]. In this paper, first we would like to analyze a potential flow around regular polygons. This can be achieved by mapping a circle to regular polygons via the Schwartz-Christoffel transformation. We then analyze triangular, diamond and hexagonal cross sections. Finally, given airfoil cross sections are studied.

II. SCHWARTZ-CHRISTOFFEL TRANSFORMATION FROM A UNIT CIRCLE TO A POLYGON

The Schwartz Christoffel transformation from a circle to a polygon can be obtained from Eq. (1) [4].

$$\frac{d\zeta}{dz} = A \prod_{j=1}^{N}\left(1 - \frac{z_j}{z}\right)^{\mu_j} = A\left(1 - \frac{e^{i\theta_1}}{z}\right)^{\mu_1}\left(1 - \frac{e^{i\theta_2}}{z}\right)^{\mu_2}..\left(1 - \frac{e^{i\theta_N}}{z}\right)^{\mu_N}.$$

(1)

Etsuo Morishita is with the Department of Advanced Interdisciplinary Sciences, Graduate School of Engineering, Utsunomiya University, 7-1-2, Yoto, Utsunomiya, Tochigi, 321-8585 Japan. phone: +81-(0)28-689-6036; fax: +81-(0)28-689-6036; e-mail: tmorisi@cc.utsunomiya-u.ac.jp/ tmorisi@mail.ecc.u-tokyo.ac.jp after April 2015.
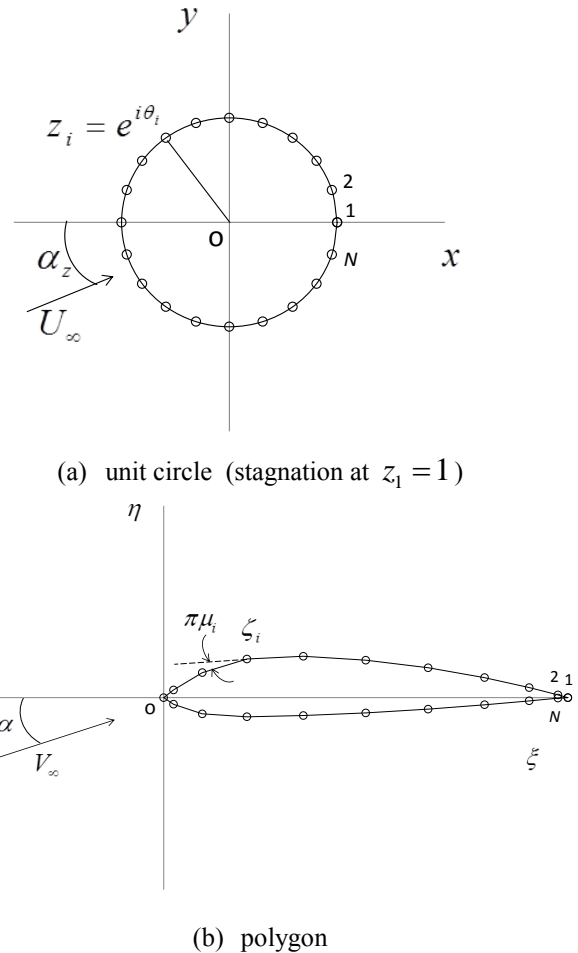

(a) unit circle (stagnation at $z_1 = 1$)

(b) polygon

Fig. 1. Schwartz-Christoffel transformation from unit circle (a) to polygon (b)

where A is a complex constant $\left(A \equiv Ke^{i\kappa}\right)$, N is the number of apexes, z is the complex coordinate of an original plane, $z_j \left(= e^{i\theta_j}, \theta_1 < \theta_2 <..<\theta_j..<\theta_N\right)$ is the j-th point on a unit circle, μ_j is the outer angular ratio to π at the j-th apex of a polygon and $\zeta \equiv \xi + i\eta$ is the transformed coordinate. A schematic view is shown in Fig. 1.

The following equations must be satisfied in Eq. (1).

$$\sum_{j=1}^{N} \mu_j = 2 . \tag{2}$$

$$\sum_{j=1}^{N} \mu_j z_j = 0 . \tag{3}$$

where Eq. (2) represents the fact that the sum of the angular rotation at each j-th apex of a polygon is equal to 2π and Eq. (3) is a necessary condition to avoid singularity by Eq.(1) and to form a closed polygon . Equation (3) becomes

$$\sum_{j=1}^{N} \mu_j \cos\theta_j = 0 . \tag{4}$$

$$\sum_{j=1}^{N} \mu_j \sin\theta_j = 0 . \tag{5}$$

In the transformed plane,

$$\frac{dw}{d\zeta}\bigg|_{|\zeta|\to\infty} = \frac{\left(\dfrac{dw}{dz}\right)_\infty}{\left(\dfrac{d\zeta}{dz}\right)_\infty} = \frac{U_\infty e^{-i\alpha_z}}{A} = \left(\frac{U_\infty}{K}\right) e^{-i(\alpha_z+\kappa)} \equiv V_\infty e^{-i\alpha} . \tag{6}$$

Therefore the uniform velocity V_∞ and the angle of attack α in the transformed plane becomes respectively as follows where K and κ are both real constants.

$$V_\infty = \frac{U_\infty}{K} . \tag{7}$$

$$\alpha = \alpha_z + \kappa . \tag{8}$$

Equation (1) becomes on the unit circle $z = e^{i\theta}$ as follows.

$$d\zeta = A \cdot 2^2 \cdot e^{i\frac{3}{2}\pi} \cdot e^{i\frac{1}{2}(\mu_1\theta_1+\mu_2\theta_2+...\mu_N\theta_N)} \cdot \left(\sin\frac{\theta_1-\theta}{2}\right)^{\mu_1}$$
$$\cdot \left(\sin\frac{\theta_2-\theta}{2}\right)^{\mu_2} \cdot ... \cdot \left(\sin\frac{\theta_N-\theta}{2}\right)^{\mu_N} d\theta \qquad . \tag{9}$$

The surface velocity on the polygon is given by

$$\frac{dw}{d\zeta} = \frac{\left(\dfrac{dw}{dz}\right)}{\left(\dfrac{d\zeta}{dz}\right)}\bigg|_{z=e^{i\theta}}$$

$$= \frac{U_\infty e^{-i\alpha_z} - \dfrac{U_\infty}{z^2 e^{-i\alpha_z}} + i\dfrac{\Gamma}{2\pi z}\bigg|_{z=e^{i\theta}}}{\left[A \cdot \dfrac{2^2 i^2}{e^{i\theta}} e^{i\frac{1}{2}(\mu_1\theta_1+\mu_2\theta_2+...\mu_N\theta_N)} \cdot \left(\sin\dfrac{\theta_1-\theta}{2}\right)^{\mu_1} \cdot \left(\sin\dfrac{\theta_2-\theta}{2}\right)^{\mu_2} \cdot ... \cdot \left(\sin\dfrac{\theta_N-\theta}{2}\right)^{\mu_N} \right]} .$$

where the circulation becomes

$$\Gamma = 4\pi U_\infty \sin\alpha_z . \tag{10}$$

and we get

$$\frac{\left(\dfrac{dw}{d\zeta}\right)}{V_\infty} = \frac{\sin(\theta-\alpha_z)+\sin\alpha_z}{\left[2 \cdot e^{i\kappa} \cdot e^{i\frac{\pi}{2}} \cdot e^{i\frac{1}{2}(\mu_1\theta_1+\mu_2\theta_2+...\mu_N\theta_N)} \cdot \left(\sin\dfrac{\theta_1-\theta}{2}\right)^{\mu_1} \cdot \left(\sin\dfrac{\theta_2-\theta}{2}\right)^{\mu_2} \cdot ... \cdot \left(\sin\dfrac{\theta_N-\theta}{2}\right)^{\mu_N} \right]} \tag{11}$$

The surface pressure coefficient is readily available from .

$$C_p = 1 - \frac{\left|\dfrac{dw}{d\zeta}\right|^2}{V_\infty^2} . \tag{12}$$

Lift and moment can be calculated theoretically from the Blasius theorems. Numerical summation is also possible.

III. REGULAR POLYGONS

A. Flat Plate

It is not common to call a flat plate a polygon, but in the present context a flat plate can be regarded the first polygon (equilateral bi-angle). We may put

$$\theta_1 = 0 . \tag{13}$$

$$\theta_2 = \pi . \tag{14}$$

$$\mu_1 = \mu_2 = 1 . \tag{15}$$

Therefore Schwartz-Christoffel transformation becomes

$$d\zeta = -2A\sin\theta \, d\theta .$$
$$\zeta = 2A\cos\theta \quad (0 \le \theta \le 2\pi) \tag{16}$$

Integral constant is taken to be zero in Eq. (16). We can set the complex constant $A \equiv Ke^{i\kappa} = K \, (\kappa = 0)$ and

$$\zeta = \xi = K\cos\theta \quad (-K \le \xi \le K) . \tag{17}$$

Equation (17) represents a flat plate in the ζ-plane.

The complex conjugate velocity is given by

$$\frac{\left(\dfrac{dw}{d\zeta}\right)}{V_\infty} = \frac{\sin(\theta-\alpha_z)+\sin\alpha_z}{\sin\theta} . \tag{18}$$

The Schwartz-Christoffel transformation includes the simplest case of the Joukowsky transformation [5]. A normal flat plate can be analyzed similarly.

B. Regular Triangle

Regular triangle case 1. A unit circle is transformed to a regular triangle by

$$\mu_1 + \mu_2 + \mu_3 = 2 . \tag{19}$$

$$\mu_1\cos\theta_1 + \mu_2\cos\theta_2 + \mu_3\cos\theta_3 = 0 . \tag{20}$$

$$\mu_1\sin\theta_1 + \mu_2\sin\theta_2 + \mu_3\sin\theta_3 = 0 . \tag{21}$$

We may choose the next three points on the unit circle.

$$\theta_1 = 0 \quad \theta_2 = \frac{2}{3}\pi \quad \theta_3 = -\frac{2}{3}\pi. \tag{22}$$

Equations (20) and (21) becomes

$$\mu_1 - \frac{1}{2}\mu_2 - \frac{1}{2}\mu_3 = 0.$$

$$0 \cdot \mu_1 + \frac{\sqrt{3}}{2}\mu_2 - \frac{\sqrt{3}}{2}\mu_3 = 0.$$

With Eq.(19), we get

$$\mu_1 = \mu_2 = \mu_3 = \frac{2}{3}. \tag{23}$$

The Schwartz-Christoffel transformation on the unit circle is

$$\frac{d\zeta}{dz} = \frac{A \cdot 2^{\frac{2}{3}} i^{\frac{2}{3}} \left(\sin\frac{3}{2}\theta \right)^{\frac{2}{3}}}{e^{i\theta}}.$$

$$d\zeta = A \cdot 2^{\frac{2}{3}} \left(\sin\frac{3}{2}\theta \right)^{\frac{2}{3}} i^{\frac{5}{3}} d\theta. \tag{24}$$

To form a regular triangle, one may put one of the three apexes at

$$\zeta = \zeta_1 = (1,0). \tag{25}$$

In this particular example, Eq.(25) represents the rear stagnation point. The rest of the remaining apexes can be at

$$\zeta_2 = \left(-\frac{1}{2}, \frac{\sqrt{3}}{2} \right). \tag{26}$$

$$\zeta_3 = \left(-\frac{1}{2}, -\frac{\sqrt{3}}{2} \right). \tag{27}$$

The side length of the regular triangle becomes $l = \sqrt{3}$.

Equation (24) is integrated numerically from ζ_1 to $\zeta_2 \left(0 \le \theta \le \frac{2\pi}{3} \right)$ as follows.

$$\zeta_2 - \zeta_1 = e^{i\kappa} \cdot e^{i\frac{5}{6}\pi} \cdot \left[K \cdot 2^{\frac{2}{3}} \cdot \int_{\theta_1}^{\theta_2} \left(\sin\frac{3}{2}\theta \right)^{\frac{2}{3}} d\theta \right] = l \cdot e^{i\frac{5}{6}\pi}. \tag{28}$$

In this integration, $\sin\frac{3}{2}\theta \ge 0$ and ζ must be on a straight line with inclination angle $5\pi/6$ relative to the ξ axis. From these conditions, we have

$$\kappa = 0. \tag{29}$$

$$K = \frac{l}{2^{\frac{2}{3}} \cdot \int_{\theta_1}^{\theta_2} \left(\sin\frac{3}{2}\theta \right)^{\frac{2}{3}} d\theta}. \tag{30}$$

In the integration from ζ_2 to ζ_3 $(2\pi/3 \le \theta \le 2 \times 2\pi/3)$, Eq.(24) must be

$$d\zeta = K \cdot e^{i\kappa} \cdot e^{i\frac{5}{6}\pi} \cdot (-1)^{\frac{2}{3}} \cdot K \cdot 2^{\frac{2}{3}} \left(-\sin\frac{3}{2}\theta \right)^{\frac{2}{3}} \cdot d\theta. \tag{31}$$

Also for ζ_3 to ζ_1 $(2 \times 2\pi/3 \le \theta \le 2\pi)$,

$$d\zeta = K \cdot e^{i\kappa} \cdot e^{i\frac{\pi}{6}} \cdot (-1)^{\frac{4}{3}} \cdot \left(\sin\frac{3}{2}\theta \right)^{\frac{2}{3}} \cdot d\theta \tag{32}$$

The complex conjugate velocity along the side of the regular triangle in the transformed plane is $(\alpha = \alpha_z + \kappa = \alpha_z)$ (Fig. 2)

$$\frac{\left(\frac{dw}{d\zeta} \right)}{V_\infty} = \frac{\left(\frac{dw}{d\zeta} \right)}{\left(\frac{U_\infty}{K} \right)} = 2^{\frac{1}{3}} \cdot \frac{\sin(\theta - \alpha) + \sin\alpha}{\left(\sin\frac{3}{2}\theta \right)^{\frac{2}{3}}} \cdot e^{i\frac{\pi}{6}}. \tag{33}$$

In Eq.(33),

$$\sin\frac{3}{2}\theta = \sin\frac{3}{2}\theta \qquad \left(0 \le \theta \le \frac{2\pi}{3} \right)$$

$$= (-1) \cdot \left(-\sin\frac{3}{2}\theta \right) \quad \left(\frac{2\pi}{3} \le \theta \le 2 \times \frac{2\pi}{3} \right).$$

$$= (-1)^2 \cdot \left(\sin\frac{3}{2}\theta \right) \quad \left(2 \times \frac{2\pi}{3} \le \theta \le 2\pi \right) \tag{34}$$

Regular triangle case 2. We may select in Eqs. (19)~(21)

$$\theta_1 = -\frac{\pi}{3}, \theta_2 = \frac{\pi}{3}, \theta_3 = \pi. \tag{35}$$

Then

$$\mu_1 \frac{1}{2} + \mu_2 \cdot \frac{1}{2} - \mu_3 = 0.$$

$$-\mu_2 \cdot \frac{\sqrt{3}}{2} + \mu_3 \cdot \frac{\sqrt{3}}{2} = 0.$$

So we get

$$\mu_1 = \mu_2 = \mu_3 = \frac{2}{3}.$$

Therefore

$$\frac{d\zeta}{dz} = A 2^{\frac{2}{3}} \left(\cos\frac{3}{2}\theta \right)^{\frac{2}{3}} e^{-i\theta}.$$

$$d\zeta = A e^{i\frac{\pi}{2}} 2^{\frac{2}{3}} \left(\cos\frac{3}{2}\theta \right)^{\frac{2}{3}} d\theta. \tag{36}$$

We may choose three apexes in the transformed plane for $l = \sqrt{3}$ as follows.

$$\zeta_1 = \left(\frac{1}{2}, -\frac{\sqrt{3}}{2} \right).$$

$$\zeta_2 = \left(\frac{1}{2}, +\frac{\sqrt{3}}{2} \right).$$

$$\zeta_3 = (-1,0).$$

We integrate from ζ_1 to ζ_2 and the argument must equal to $\pi/2$. This means

$$\zeta_2 - \zeta_1 = \left[K \cdot 2^{\frac{2}{3}} \cdot \int_{\theta_1}^{\theta_2} \left(\cos\frac{3}{2}\theta \right)^{\frac{2}{3}} d\theta \right] \cdot e^{i\kappa} \cdot e^{i\frac{\pi}{2}} \cdot = l \cdot e^{i\frac{\pi}{2}}. \qquad (37)$$

We get therefore

$$\kappa = 0. \qquad (38)$$

$$K = \frac{l}{2^{\frac{2}{3}} \cdot \int_{\theta_1}^{\theta_2} \left(\cos\frac{3}{2}\theta \right)^{\frac{2}{3}} d\theta}. \qquad (39)$$

The complex conjugate velocity is given by (see Fig. 2, lateral coordinate inverted.)

$$\frac{\left(\dfrac{dw}{d\zeta} \right)}{V_\infty} = 2^{\frac{1}{3}} \cdot \frac{\sin(\theta-\alpha)+\sin\alpha}{\left(\cos\dfrac{3}{2}\theta \right)^{\frac{2}{3}}} \cdot e^{i\frac{\pi}{2}}. \qquad (40)$$

The denominator must be interpreted as follows.

$$\left(\cos\frac{3}{2}\theta \right)^{\frac{2}{3}} = \left(\cos\frac{3}{2}\theta \right)^{\frac{2}{3}} \quad \left(-\frac{\pi}{3} \leq \theta \leq \frac{\pi}{3} \right)$$

$$= (-1)^{\frac{2}{3}}\left(-\cos\frac{3}{2}\theta \right)^{\frac{2}{3}} \left(\frac{\pi}{3} \leq \theta \leq \pi \right) . \qquad (41)$$

$$= (-1)^{\frac{4}{3}}\left(-\cos\frac{3}{2}\theta \right)^{\frac{2}{3}} \left(\pi \leq \theta \leq \frac{5\pi}{3} \right)$$
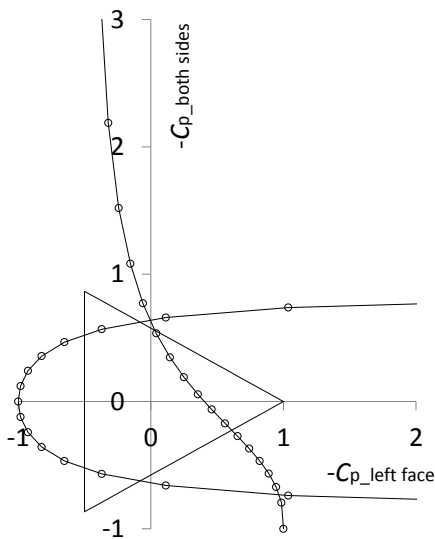

Fig. 2. Regular triangle $-C_p$
(case 1/case 2, uniform flow either from left or right)

C. Square

Square case 1. We can imagine from preceding examples that

$$\theta_i = \frac{\pi}{2}(i-1) \quad (1 \leq i \leq 4). \qquad (42)$$

$$\mu_i = \frac{1}{2} \quad (1 \leq i \leq 4). \qquad (43)$$

We have therefore on the unit circle

$$\frac{d\zeta}{dz} = A(2i)^{\frac{1}{2}} \frac{(\sin 2\theta)^{\frac{1}{2}}}{e^{i\theta}}. \qquad (44)$$

$$d\zeta = A \cdot 2^{\frac{1}{2}} \cdot i^{\frac{3}{2}} \cdot (\sin 2\theta)^{\frac{1}{2}} \cdot d\theta. \qquad (45)$$

We choose for a square with the side length $l = \sqrt{2}$ as follows.

$$\zeta_1 = (1,0), \quad \zeta_2 = (0,1), \quad \zeta_3 = (-1,0), \quad \zeta_4 = (0,-1)$$

Integration from ζ_1 to ζ_2 is on the straight line and

$$\zeta_2 - \zeta_1 = \left[K \cdot 2^{\frac{1}{2}} \cdot \int_{\theta_1}^{\theta_1} (\sin 2\theta)^{\frac{1}{2}} \cdot d\theta \right] \cdot e^{i\kappa} \cdot e^{i\frac{3}{4}\pi} = l \cdot e^{i\frac{3}{4}\pi}. \qquad (46)$$

We therefore get

$$K = \frac{l}{2^{\frac{1}{2}} \cdot \int_{\theta_1}^{\theta_2} (\sin 2\theta)^{\frac{1}{2}} \cdot d\theta}. \qquad (47)$$

$$\kappa = 0. \qquad (48)$$

The complex conjugate velocity along the square surface is obtained as follows (see Fig. 3).

$$\frac{\left(\dfrac{dw}{d\zeta} \right)}{V_\infty} = 2^{\frac{1}{2}} \cdot \frac{\sin(\theta-\alpha)+\sin\alpha}{(\sin 2\theta)^{\frac{1}{2}}} \cdot e^{i\frac{\pi}{4}}. \qquad (49)$$
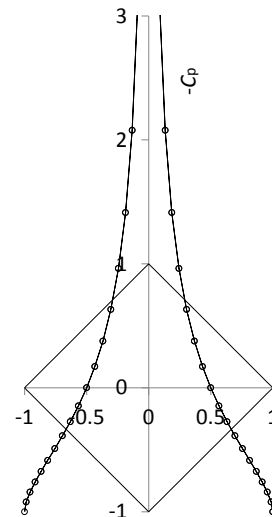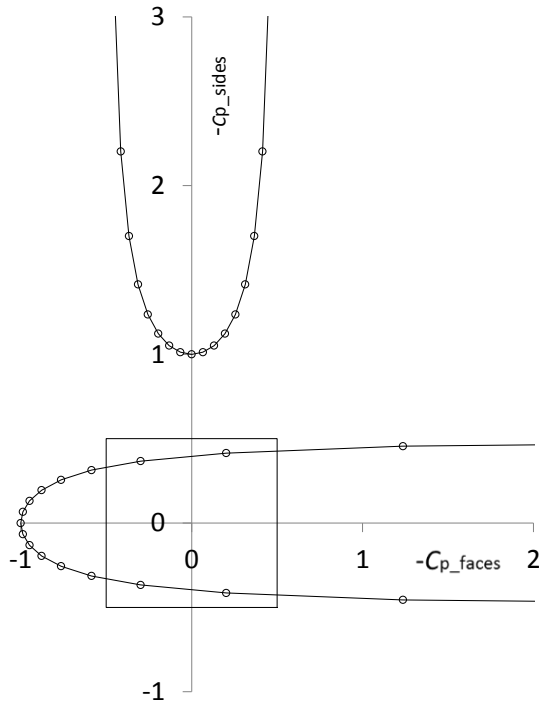

Fig.3. Square (case 1) $-C_p$

Fig. 4. Square (case 2) $-C_p$
(uniform flow either from left or right in Figs. 3 and 4)

The denominator is treated in the same manner as that of the regular triangle.

Square case 2.   We can imagine from preceding examples that

$$\theta_i = -\frac{\pi}{4} + \frac{\pi}{2}(i-1) \quad (1 \le i \le 4).$$ (50)

$$\mu_i = \frac{1}{2} \quad (1 \le i \le 4).$$ (51)

We have therefore on the unit circle

$$\frac{d\zeta}{dz} = A \frac{2^{\frac{1}{2}}(\cos 2\theta)^{\frac{1}{2}}}{e^{i\theta}} \cdot$$ (52)

$$d\zeta = A 2^{\frac{1}{2}} e^{i\frac{\pi}{2}} (\cos 2\theta)^{\frac{1}{2}} d\theta \cdot$$ (53)

We may choose for $l = \sqrt{2}$ as follows.

$$\zeta_1 = \left(\frac{1}{\sqrt{2}}, -\frac{1}{\sqrt{2}}\right), \quad \zeta_2 = \left(\frac{1}{\sqrt{2}}, \frac{1}{\sqrt{2}}\right),$$

$$\zeta_3 = \left(-\frac{1}{\sqrt{2}}, \frac{1}{\sqrt{2}}\right), \quad \zeta_4 = \left(-\frac{1}{\sqrt{2}}, -\frac{1}{\sqrt{2}}\right).$$

Integrate from ζ_1 to ζ_2 and the path is vertical.

$$\zeta_2 - \zeta_1 = \left[K \cdot 2^{\frac{1}{2}} \cdot \int_{\theta_1}^{\theta_1} (\cos 2\theta)^{\frac{1}{2}} d\theta \right] \cdot e^{i\kappa} \cdot e^{i\frac{\pi}{2}} = l \cdot e^{i\frac{\pi}{2}}.$$ (54)

Then we have

$$K = \frac{l}{2^{\frac{1}{2}} \cdot \int_{\theta_1}^{\theta_1} (\cos 2\theta)^{\frac{1}{2}} d\theta} \cdot$$ (55)

$$\kappa = 0.$$ (56)

The complex conjugate velocity becomes (see Fig. 4)

$$\frac{\left(\frac{dw}{d\zeta}\right)}{V_\infty} = 2^{\frac{1}{2}} \cdot \frac{\sin(\theta - \alpha) + \sin\alpha}{(\cos 2\theta)^{\frac{1}{2}}} \cdot e^{i\frac{\pi}{2}}.$$ (57)

D.   General Regular Polygons

From above calculations, we found for regular polygons as follows (see also Ref. [5] and [6]).
For case 1 $(\theta_1 = 0)$

Flat plate $\dfrac{d\zeta}{dz} = A \dfrac{2i\sin\theta}{e^{i\theta}}.$

Regular triangle $\dfrac{d\zeta}{dz} = A \dfrac{2^{\frac{2}{3}} i^{\frac{2}{3}} \left(\sin\frac{3}{2}\theta\right)^{\frac{2}{3}}}{e^{i\theta}}.$

Square $\dfrac{d\zeta}{dz} = A \dfrac{2^{\frac{1}{2}} i^{\frac{1}{2}} (\sin 2\theta)^{\frac{1}{2}}}{e^{i\theta}}.$

For case 2 $\left(\theta_1 = -\pi/n\right)$

Flat plate $\dfrac{d\zeta}{dz} = A \dfrac{2\cos\theta}{e^{i\theta}}.$

Regular triangle $\dfrac{d\zeta}{dz} = A \dfrac{2^{\frac{2}{3}}}{e^{i\theta}} \left(\cos\frac{3}{2}\theta\right)^{\frac{2}{3}}.$

Square $\dfrac{d\zeta}{dz} = A \dfrac{2^{\frac{1}{2}} (\cos 2\theta)^{\frac{1}{2}}}{e^{i\theta}}.$

Then we can assume for n-th regular polygon for $\theta_1 = 0$

$$\frac{d\zeta}{dz} = A \frac{2^{\frac{2}{n}} i^{\frac{2}{n}}}{e^{i\theta}} \left(\sin\frac{n}{2}\theta\right)^{\frac{2}{n}}.$$ (58)

$$\frac{\left(\frac{dw}{d\zeta}\right)}{V_\infty} = 2^{1-\frac{2}{n}} \cdot i^{1-\frac{2}{n}} \cdot \frac{\sin(\theta - \alpha) + \sin\alpha}{\left(\sin\frac{n}{2}\theta\right)^{\frac{2}{n}}}.$$ (59)

For a n-th regular polygon for $\theta_1 = -\pi/n$

$$\frac{d\zeta}{dz} = A \frac{2^{\frac{2}{n}} \left(\cos\frac{n}{2}\theta\right)^{\frac{2}{n}}}{e^{i\theta}}.$$ (60)

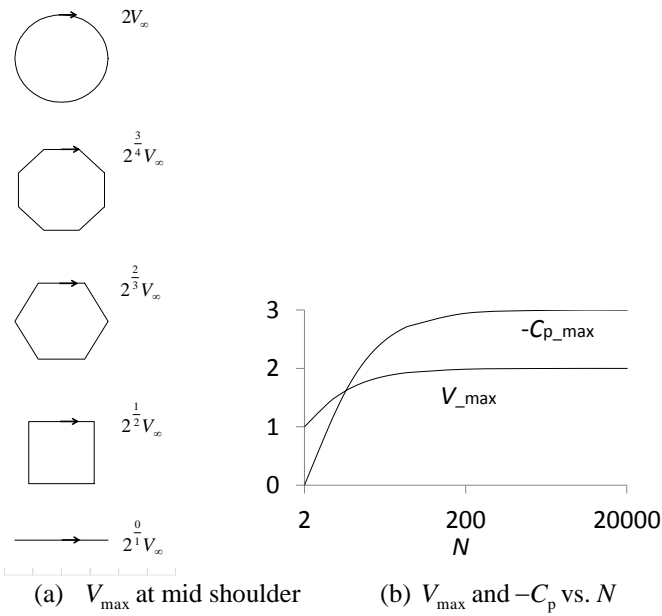(a) $V_{\max}$ at mid shoulder   (b) $V_{\max}$ and $-C_p$ vs. N

Fig. 5. Regular polygons with even sides $N = 2m\,(m = 1,2,3,\ldots)$
(cf. Eq. (2.6) of Ref. [6])

$$\frac{\left(\dfrac{dw}{d\zeta}\right)}{V_\infty} = 2^{1-\frac{2}{n}} \cdot i \cdot \frac{\sin(\theta - \alpha) + \sin\alpha}{\left(\cos\dfrac{n}{2}\theta\right)^{\frac{2}{n}}} . \qquad (61)$$

In the present setting, $A = K$ and $\kappa = 0$.

It is very interesting to note that the maximum velocity (maximum for a circular cylinder only) at the shoulder side surface parallel to the uniform flow is given by equation below for regular polygons for $n = 2,4,6,8,\ldots 2m,\ldots$, where m is an integer (cf. Eq. (2.6) of Ref. [6]).

$$\frac{\left(\dfrac{dw}{d\zeta}\right)}{V_\infty} = 2^{1-\frac{2}{n}} . \qquad (62)$$

The specific value becomes

$2^{\frac{0}{1}}$ for a flat plate $(n = 2)$,

$2^{\frac{1}{2}}$ for a square $(n = 4)$,

$2^{\frac{2}{3}}$ for a hexagon $(n = 6)$,

$2^{\frac{3}{4}}$ for an octagon $(n = 8)$,

…

$2^{\frac{m-1}{m}}$ for an general regular polygon

with even sides $(n = 2m)$.

Note that the power is rather striking, and 2 for a circle $(n \to \infty)$.

IV.   POLYGON AIRFOIL SECTIONS

A.   Triangular Airfoil Section

For a triangular airfoil, we get

$$\mu_1 + \mu_2 + \mu_3 = 2 . \qquad (63)$$

$$\mu_1 \cos\theta_1 + \mu_2 \cos\theta_2 + \mu_3 \cos\theta_3 = 0 . \qquad (64)$$

$$\mu_1 \sin\theta_1 + \mu_2 \sin\theta_2 + \mu_3 \sin\theta_3 = 0 . \qquad (65)$$

For a triangle in Fig.6, we get

$$\mu_1 = \frac{\pi - \bar{\alpha}}{\pi} = 1 - \frac{\bar{\alpha}}{\pi} . \qquad (66)$$

$$\mu_2 = 1 - \frac{\bar{\beta}}{\pi} . \qquad (67)$$

$$\mu_3 = 1 - \frac{\bar{\gamma}}{\pi} = \frac{\bar{\alpha} + \bar{\beta}}{\pi} = 2 - (\mu_1 + \mu_2) . \qquad (68)$$

We can choose θ_1 arbitrary and $\theta_1 = 0$ and θ_2 and θ_3 can be determined numerically.

It can be shown that for $0 \le \theta \le \theta_2$

$$d\zeta = K \cdot 2^2 \cdot e^{i\left[\frac{3}{2}\pi + \frac{1}{2}\sum_{j=1}^{3}\mu_j \cdot \theta_j + \kappa + \mu_1\pi\right]} \cdot \prod_{j=1}^{3}\left|\sin\frac{\theta_j - \theta}{2}\right|^{\mu_j} \cdot d\theta . \quad (69)$$

and from the inclination of the first side

$$\kappa = -\left(\frac{3}{2}\pi + \frac{1}{2}\sum_{j=1}^{3}\mu_j \cdot \theta_j\right) . \qquad (70)$$

We get

$$\zeta_2 - \zeta_1 = \left[K \cdot 2^2 \cdot \int_{\theta_1}^{\theta_2} \prod_{j=1}^{3}\left|\sin\frac{\theta_j - \theta}{2}\right|^{\mu_j} \cdot d\theta\right] \cdot e^{i \cdot \mu_1 \pi}$$
$$= l_1 \cdot e^{i \cdot \mu_1 \pi} \qquad (71)$$

For $\theta_2 \le \theta \le \theta_3$

$$\zeta_3 - \zeta_2 = \left[K \cdot 2^2 \cdot \int_{\theta_2}^{\theta_3} \prod_{j=1}^{3}\left|\sin\frac{\theta_j - \theta}{2}\right|^{\mu_j} \cdot d\theta\right] \cdot e^{i(\mu_1+\mu_2)\pi}$$
$$= l_2 \cdot e^{i(\mu_1+\mu_2)\pi} \qquad (72)$$

For $\theta_3 \le \theta \le 2\pi$

$$\zeta_1 - \zeta_3 = \left[K \cdot 2^2 \cdot \int_{\theta_3}^{2\pi} \prod_{j=1}^{3}\left|\sin\frac{\theta_j - \theta}{2}\right|^{\mu_j} \cdot d\theta\right]$$
$$\cdot e^{i(\mu_1+\mu_2+\mu_3)\pi} = l_3 \qquad (73)$$

The constant K can be determined either of the above three equations.

The complex conjugate velocity is given as follows and a result for a triangular airfoil by Yonezawa et al. [7] is shown in Fig.7.

$$\frac{\left(\frac{dw}{d\zeta}\right)}{V_\infty} = \frac{1}{2}\frac{\sin(\theta-\alpha_z)+\sin\alpha_z}{\prod\limits_{j=1}^{3}\left|\sin\dfrac{\theta_j-\theta}{2}\right|^{\mu_j}} e^{i\pi-i\pi\mu_1} \quad (0\le\theta\le\theta_2). \qquad (74)$$

$$\frac{\left(\frac{dw}{d\zeta}\right)}{V_\infty} = \frac{1}{2}\frac{\sin(\theta-\alpha_z)+\sin\alpha_z}{\prod\limits_{j=1}^{3}\left|\sin\dfrac{\theta_j-\theta}{2}\right|^{\mu_j}} e^{i\pi-i\pi\mu_1-i\pi\mu_2} \quad (\theta_2\le\theta\le\theta_3). \qquad (75)$$

$$\frac{\left(\frac{dw}{d\zeta}\right)}{V_\infty} = \frac{1}{2}\frac{\sin(\theta-\alpha_z)+\sin\alpha_z}{\prod\limits_{j=1}^{3}\left|\sin\dfrac{\theta_j-\theta}{2}\right|^{\mu_j}} e^{-i\pi} \quad (\theta_3\le\theta\le2\pi). \qquad (76)$$
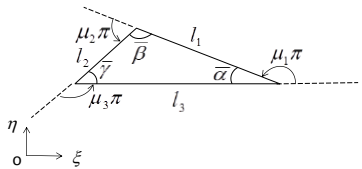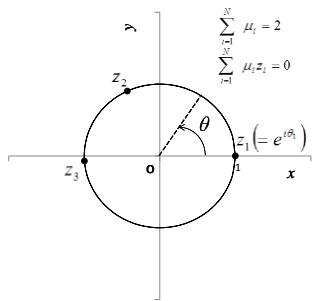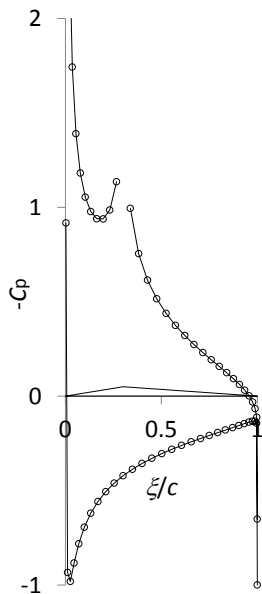

Fig. 6. Triangle generation

Fig. 7. Triangular airfoil $-C_p$ at $\alpha=8°$

$\left(t_{max}/c = 0.05\text{ at }\xi/c = 0.3\quad[7]\right)$

Equations (63), (64) and (65) could be equivalent to the geometrical conditions below.

$$\bar\alpha+\bar\beta+\bar\gamma = 2\pi. \qquad (77)$$

$$l_1\cos\bar\alpha + l_2\cos\bar\gamma = l_3. \qquad (78)$$

$$l_1\sin\bar\alpha = l_2\sin\bar\gamma. \qquad (79)$$

B. Diamond Airfoil Section

A diamond airfoil section is a very popular academic subject in high-speed aerodynamics. It may be worthwhile to investigate the low-speed characteristics of the airfoil. A symmetric diamond airfoil is analyzed as follows.

$$\mu_1+\mu_2+\mu_3+\mu_4 = 2. \qquad (80)$$

$$\mu_1\cos\theta_1 + \mu_2\cos\theta_2 + \mu_3\cos\theta_3 + \mu_4\cos\theta_4 = 0. \qquad (81)$$

$$\mu_1\sin\theta_1 + \mu_2\sin\theta_2 + \mu_3\sin\theta_3 + \mu_4\sin\theta_4 = 0. \qquad (82)$$

$$\theta_1 = 0, \theta_2 = 1\times\frac{\pi}{2}, \theta_3 = 2\times\frac{\pi}{2}, \theta_4 = 3\times\frac{\pi}{2}. \qquad (83)$$

The half apex angle is given by δ and

$$\mu_1 = \mu_2 = \frac{\pi-2\delta}{\pi} \equiv \mu. \qquad (84)$$

$$\mu_2 = \mu_4 = \frac{\pi-(\pi-2\delta)}{\pi} = 1-\mu. \qquad (85).$$

For the first panel $\theta_1(=0)\le\theta\le\theta_2$ from the trailing edge with an inclination $\pi-\delta$, we get

$$\zeta_2-\zeta_1 = \left[K\cdot2^2\cdot\int_{\theta_1}^{\theta_2}\prod_{j=1}^{4}\left|\sin\frac{\theta_j-\theta}{2}\right|^{\mu_j}\cdot d\theta\right]$$
$$\cdot e^{i\left[\kappa+\frac{3}{2}\pi+\frac{1}{2}\sum\limits_{j=1}^{4}\cdot\mu_j\cdot\theta_j+\mu_1\pi\right]} = l\cdot e^{i(\pi-\delta)} \qquad (86)$$

where

$$l = \frac{c}{2}\cdot\frac{1}{\cos\delta}. \qquad (87)$$

Therefore we get

$$K = \frac{l}{2^2\cdot\int\limits_{\theta_1}^{\theta_2}\prod\limits_{j=1}^{4}\left|\sin\dfrac{\theta_j-\theta}{2}\right|^{\mu_j}\cdot d\theta}. \qquad (88)$$

$$\kappa = \pi-\delta-\left(\frac{3}{2}\pi+\frac{1}{2}\sum_{j=1}^{4}\mu_j\theta_j+\mu_1\pi\right) = 0. \qquad (89)$$
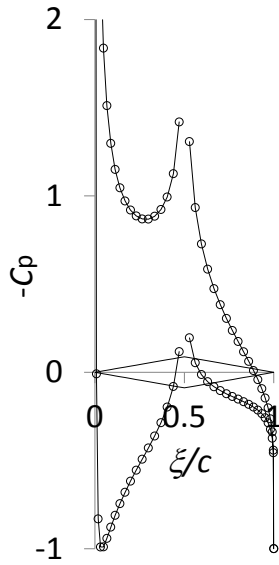
The complex conjugate velocity is given by

Fig. 8. Diamond airfoil section $-C_\mathrm{p}$ at $\alpha = 10°$, $\delta = 10°$

$$\frac{\left(\dfrac{dw}{d\zeta}\right)}{V_\infty} = \frac{\sin(\theta - \alpha_z) + \sin\alpha_z}{2\cdot e^{\left[i\cdot\left[\frac{\pi}{2}+\frac{1}{2}\sum_{j=1}^{N}\,\cdot\mu_j\cdot\theta_j+\kappa\right]\right]}\cdot\prod_{j=1}^{N}\left(\sin\dfrac{\theta_j-\theta}{2}\right)^{\mu_j}}\quad(90)$$

More specifically

$$\frac{\left(\dfrac{dw}{d\zeta}\right)}{V_\infty} = \frac{\sin(\theta - \alpha_z) + \sin\alpha_z}{2\cdot\prod_{j=1}^{N}\left|\sin\dfrac{\theta_j-\theta}{2}\right|^{\mu_j}}\cdot e^{-i\beta}\quad(91)$$

$$0 \le \theta \le \frac{\pi}{2}\quad \beta = -\delta$$

$$\frac{\pi}{2} \le \theta \le \pi\quad \beta = \delta$$

$$\pi \le \theta \le \frac{3}{2}\pi\quad \beta = \pi - \delta$$

$$\frac{3}{2}\pi \le \theta \le 2\pi\quad \beta = \pi + \delta$$

Figure 8 shows a diamond airfoil with the half apex angle $\delta = 10°$ and an angle of attack $\alpha = 10°$.

C. Rudder

A rudder problem was solved by Fukatsu [2] many decades ago and we repeat the solution here because it is one of the most beautiful solutions of the Schwartz-Christoffel transformation to the present author's knowledge.

The conditions are given as follows.

$$\mu_1 + \mu_2 + \mu_3 + \mu_4 = 2.\quad(92)$$

$$\mu_1\cos\theta_1 + \mu_2\cos\theta_2 + \mu_3\cos\theta_3 + \mu_4\cos\theta_4 = 0.\quad(93)$$

$$\mu_1\sin\theta_1 + \mu_2\sin\theta_2 + \mu_3\sin\theta_3 + \mu_4\sin\theta_4 = 0.\quad(94)$$

where

$$-\mu_1 = \mu_3 = \mu\ \left(=\frac{\delta}{\pi}\right),\quad \mu_2 = \mu_4 = 1\ \left(=\frac{\pi}{\pi}\right).\quad(95)$$

We can choose θ_1 arbitrary and we put as follows.

$$\theta_1 = -\theta_3.\quad(96)$$

From this we get

$$\theta_4 = \pi - \theta_2.\quad(97)$$

$$\mu\sin\theta_3 = \sin\theta_2.\quad(98)$$

The Schwartz-Christoffel transformation becomes

$$\frac{d\zeta}{dz} = A\cdot\left(1 - \frac{e^{-i\theta_3}}{z}\right)^{\mu}\cdot\left(1 - \frac{e^{i\theta_2}}{z}\right)$$
$$\cdot\left(1 - \frac{e^{i\theta_3}}{z}\right)^{-\mu}\cdot\left(1 - \frac{e^{i(\pi-\theta_2)}}{z}\right).\quad(99)$$

It was shown elegantly by Fukatsu that

$$\frac{d}{dz}A\cdot z\cdot\left(1 - \frac{e^{-i\theta_3}}{z}\right)^{1+\mu}\cdot\left(1 - \frac{e^{i\theta_3}}{z}\right)^{1-\mu}.\quad(100)$$

$$= A\cdot\left(1 - \frac{e^{-i\theta_3}}{z}\right)^{\mu}\cdot\left(1 - \frac{e^{i\theta_3}}{z}\right)^{-\mu}$$
$$\times\left(1 - \frac{e^{i\theta_2}}{z}\right)\cdot\left(1 - \frac{e^{-i(\pi-\theta_2)}}{z}\right)$$

We therefore get a closed analytical solution in this case.

$$\zeta = Az\left(1 - \frac{e^{-i\theta_3}}{z}\right)^{1+\mu}\left(1 - \frac{e^{i\theta_3}}{z}\right)^{1-\mu} + B.\quad(101)$$

We may choose the root of the rudder locates at the origin

$$\zeta = \zeta(z_1) = \zeta(z_3) = 0\ \left(z_1 = e^{i\theta_1} = e^{-i\theta_3} = z_3\right).\quad(102)$$

and therefore $B = 0$. Equation (101) can be simplified as follows.

$$\zeta = \left[K\cdot 2^2\cdot\left(\sin\frac{\theta+\theta_3}{2}\right)^{1+\mu}\cdot\left(\sin\frac{\theta-\theta_3}{2}\right)^{1-\mu}\right]$$
$$\cdot e^{i\pi}\cdot e^{i(\kappa-\mu\theta_3)}\quad(103)$$

The leading edge locates at $\theta = \theta_4 = \pi - \theta_2$ and

$$\zeta_{l.e.} = l\cdot e^{i\pi}$$
$$= \left[K\cdot 2^2\left(\cos\frac{\theta_3-\theta_2}{2}\right)^{1+\mu}\cdot\left(\cos\frac{\theta_3+\theta_2}{2}\right)^{1-\mu}\right]$$
$$\cdot e^{i\pi}\cdot e^{i(\kappa-\mu\theta_3)}\quad(104)$$

So we can determine κ and l as follows.

$$\kappa = \mu\theta_3 .$$ (105)

$$l = 2^2 \cdot K \cdot \left(\cos\frac{\theta_3 - \theta_2}{2}\right)^{1+\mu} \cdot \left(\cos\frac{\theta_3 + \theta_2}{2}\right)^{1-\mu} .$$ (106)

The trailing edge locates at $\theta = \theta_2$ and

$$\zeta_{t.e.} = l' \cdot e^{-i\delta} = K \cdot 2^2 \cdot \left(\sin\frac{\theta_3 + \theta_2}{2}\right)^{1+\mu}$$
$$\cdot \left(\sin\frac{\theta_3 - \theta_2}{2}\right)^{1-\mu} \cdot e^{i\pi(1-\mu)} \cdot e^{i\pi}$$ (107)

$$l' = K \cdot 2^2 \cdot \left(\sin\frac{\theta_3 + \theta_2}{2}\right)^{1+\mu} \left(\sin\frac{\theta_3 - \theta_2}{2}\right)^{1-\mu} .$$ (108)

The circulation is determined by the fact the trailing edge is the rear stagnation point and we have

$$\Gamma = 4\pi U_\infty (\alpha_z - \theta)\big|_{\theta=\theta_2} = 4\pi U_\infty (\alpha_z - \theta_2) .$$ (109)

The final form of the complex conjugate velocity is given by

$$\frac{\left(\dfrac{dw}{d\zeta}\right)}{V_\infty} = \frac{\sin(\theta - \alpha_z) - \sin(\theta_2 - \alpha_z)}{\sin\theta - \sin\theta_2} \cdot \frac{\left(\sin\dfrac{\theta - \theta_3}{2}\right)^\mu}{\left(\sin\dfrac{\theta + \theta_3}{2}\right)^\mu} .$$ (110)

We repeat

$$\alpha = \alpha_z + \kappa$$

$$V_\infty = \frac{U_\infty}{K} .$$

$$\Gamma = 4\pi K V_\infty \sin(\alpha - \kappa - \theta_2) .$$

$$C_l = \frac{\rho V_\infty \times 4\pi K V_\infty \sin(\alpha - \kappa - \theta_2)}{\frac{1}{2}\rho V_\infty^2 \times c} = \frac{8\pi K}{c} \cdot \sin(\alpha - \kappa - \theta_2) .$$

The chord length may be defined as follows.

$$c = l + l'$$
$$= K \cdot 2^2 \cdot \left(\cos\frac{\theta_3 - \theta_2}{2}\right)^{1+\mu} \cdot \left(\cos\frac{\theta_3 + \theta_2}{2}\right)^{1-\mu}$$
$$+ K \cdot 2^2 \cdot \left(\sin\frac{\theta_3 + \theta_2}{2}\right)^{1+\mu} \cdot \left(\sin\frac{\theta_3 - \theta_2}{2}\right)^{1-\mu} .$$ (111)
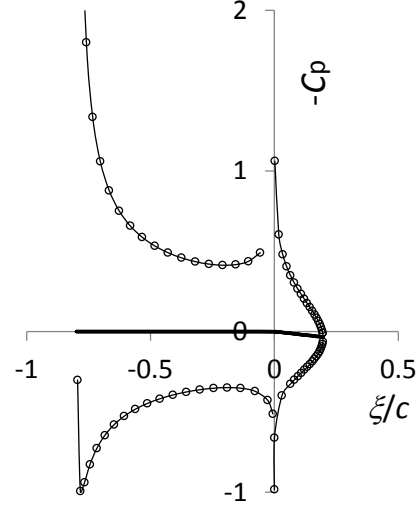
The lift coefficient is given by

Fig. 9. Rudder analytical solution $-C_p$ at $\alpha = 5°$, $\delta = -10°$

$$C_l = \frac{2\pi \cdot \sin(\alpha - \kappa - \theta_2)}{\left[\left(\cos\dfrac{\theta_3 - \theta_2}{2}\right)^{1+\mu} \cdot \left(\cos\dfrac{\theta_3 + \theta_2}{2}\right)^{1-\mu}\right. }{\left. + \left(\sin\dfrac{\theta_3 + \theta_2}{2}\right)^{1+\mu} \cdot \left(\sin\dfrac{\theta_3 - \theta_2}{2}\right)^{1-\mu}\right]} .$$ (112)

A good approximation is

$$C_l \approx 2\pi \sin(\alpha - \kappa - \theta_2) = 2\pi(\alpha - \mu\theta_3 - \mu\sin\theta_3) .$$ (113)

The rudder length to chord ratio is given by

$$\frac{l'}{c} = \frac{\left(\sin\dfrac{\theta_3 + \theta_2}{2}\right)^{1+\mu} \cdot \left(\sin\dfrac{\theta_3 - \theta_2}{2}\right)^{1-\mu}}{\left[\left(\cos\dfrac{\theta_3 - \theta_2}{2}\right)^{1+\mu} \cdot \left(\cos\dfrac{\theta_3 + \theta_2}{2}\right)^{1-\mu}\right.}{\left. + \left(\sin\dfrac{\theta_3 + \theta_2}{2}\right)^{1+\mu} \cdot \left(\sin\dfrac{\theta_3 - \theta_2}{2}\right)^{1-\mu}\right]} .$$ (114)

We can determine θ_2 and θ_3 numerically for a given l'/c together with the relationship $\mu\sin\theta_3 = \sin\theta_2$. From these angles, we can finally obtain θ_1 and θ_4, then the problem is solved. A rudder with $\delta = -10°$ at $a = 10°$ is shown in Fig. 9.

D. Hexagonal Airfoil Section

A symmetric hexagonal airfoil is used as a stabilizer and the general relationship becomes as follows.

$$\mu_1 + \mu_2 + \mu_3 + \mu_4 + \mu_5 + \mu_6 = 2 .$$ (115)
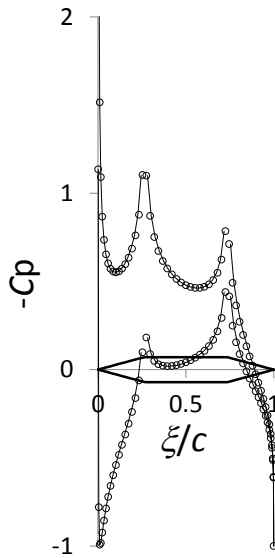
Fig.10. Hexagonal airfoil $-C_p$ at $\alpha = 5^\circ$, $\delta = 15^\circ$

$$\mu_1 \cos\theta_1 + \mu_2 \cos\theta_2 + \mu_3 \cos\theta_3$$
$$+ \mu_4 \cos\theta_4 + \mu_5 \cos\theta_5 + \mu_6 \cos\theta_6 = 0 \qquad (116)$$

$$\mu_1 \sin\theta_1 + \mu_2 \sin\theta_2 + \mu_3 \sin\theta_3$$
$$+ \mu_4 \sin\theta_4 + \mu_5 \sin\theta_5 + \mu_6 \sin\theta_6 = 0 \qquad (117)$$

We may put

$$\theta_1 = 0, \theta_2 = \chi, \theta_3 = \pi - \chi,$$
$$\theta_4 = \pi, \theta_5 = \pi + \chi, \theta_6 = 2\pi - \chi \qquad (118)$$

A half apex angle is δ and we get

$$\mu_1 = \mu_4 = \frac{\pi - 2 \times \delta}{\pi} = 1 - 2\frac{\delta}{\pi} \qquad (119)$$

$$\mu_2 = \mu_3 = \mu_5 = \mu_6 = \frac{\delta}{\pi} \qquad (120)$$

$$l_1 = l_3 = l_4 = l_6 \equiv l \qquad (121)$$

$$l_2 = l_5 = c - 2 \cdot l \cdot \cos\delta \qquad (122)$$

For the first panel

$$\zeta_2 - \zeta_1 = \left[K \cdot 2^2 \cdot \int_{\theta_1}^{\theta_2} \prod_{j=1}^{6} \left| \sin\frac{\theta_j - \theta}{2} \right|^{\mu_j} \cdot d\theta \right].$$
$$\cdot e^{i\left[\kappa + \frac{3}{2}\pi + \frac{1}{2}\sum_{j=1}^{6} \cdot \mu_j \cdot \theta_j + \mu_1\pi \right]} = l \cdot e^{i(\pi - \delta)} \qquad (123)$$

We can show that

$$K = \frac{l}{2^2 \cdot \int_{\theta_1}^{\theta_2} \prod_{j=1}^{6} \left| \sin\frac{\theta_j - \theta}{2} \right|^{\mu_j} \cdot d\theta} \qquad (124)$$

$$\kappa = 0 \qquad (125)$$

where we use

$$\sum_{j=1}^{6} \mu_j \theta_j = \pi + 2\delta \qquad (126)$$

The complex conjugate velocity is given by (see Fig.10 for $\delta = 15^\circ$ at $\alpha = 5^\circ$)

$$\frac{\left(\dfrac{dw}{d\zeta}\right)}{V_\infty} = \frac{\sin(\theta - \alpha_z) + \sin\alpha_z}{2 \cdot \prod\limits_{j=1}^{N} \left| \sin\dfrac{\theta_j - \theta}{2} \right|^{\mu_j}} \cdot e^{-i\beta} \qquad (127)$$

$$\begin{aligned}
0 \le \theta \le \chi & \qquad \beta = -\delta \\
\chi \le \theta \le \pi - \chi & \qquad \beta = 0 \\
\pi - \chi \le \theta \le \pi & \qquad \beta = \delta \\
\pi \le \theta \le \pi + \chi & \qquad \beta = \pi - \delta \\
\pi + \chi \le \theta \le 2\pi - \chi & \qquad \beta = \pi \\
2\pi - \chi \le \theta \le 2\pi & \qquad \beta = \pi + \delta
\end{aligned}$$

V. GIVEN AIRFOIL SECTIONS

A given airfoil was analyzed by the Schwartz-Cristoeffel transformation and it may be called the Schwartz-Christoffel panel method [2]. The method is repeated here in a more simpler procedure than that of the original one.

An airfoil is approximated by *N* panels and along the panel surface

$$d\zeta = K \cdot 2^2 \cdot e^{i\left[\frac{3}{2}\pi + \frac{1}{2}\sum_{j=1}^{N} \cdot \mu_j \cdot \theta_j + \kappa\right]} \cdot \prod_{j=1}^{N} \left(\sin\frac{\theta_j - \theta}{2} \right)^{\mu_j} \cdot d\theta \qquad (128)$$

We can imagine that for $j = i$ $(\theta_i \le \theta \le \theta_{i+1})$

$$d\zeta = K \cdot 2^2 \cdot e^{i\left[\frac{3}{2}\pi + \frac{1}{2}\sum_{j=1}^{N} \cdot \mu_j \cdot \theta_j + \kappa\right]} \cdot (-1)^{\mu_1} \cdot (-1)^{\mu_2} \cdots (-1)^{\mu_i}$$
$$\times \prod_{j=i+1}^{N} \left| \sin\frac{\theta_1 - \theta}{2} \right|^{\mu_1} \cdot \left| \sin\frac{\theta_2 - \theta}{2} \right|^{\mu_2} \cdots \left| \sin\frac{\theta_i - \theta}{2} \right|^{\mu_i}$$
$$\cdot \left(\sin\frac{\theta_j - \theta}{2} \right)^{\mu_j} \cdot d\theta \qquad (129)$$

From these equations, for the panel *i*

$$\zeta_{i+1} - \zeta_i = \left[K \cdot 2^2 \cdot \int_{\theta_i}^{\theta_{i+1}} \prod_{j=1}^{N} \left| \sin\frac{\theta_j - \theta}{2} \right|^{\mu_j} \cdot d\theta \right].$$
$$\cdot e^{i\left[\frac{3}{2}\pi + \frac{1}{2}\sum_{j=1}^{N} \cdot \mu_j \cdot \theta_j + \kappa + \pi\sum_{j=1}^{i}\mu_j\right]} \equiv l_i \cdot e^{i\delta_i} \qquad (130)$$

where

$$l_i \equiv K \cdot 2^2 \cdot \int_{\theta_i}^{\theta_{i+1}} \prod_{j=1}^{N} \left| \sin\frac{\theta_j - \theta}{2} \right|^{\mu_j} \cdot d\theta \quad (1 \le i \le N) \qquad (131)$$

and

$$\delta_i \equiv \frac{3}{2}\pi + \frac{1}{2}\sum_{j=1}^{N} \cdot \mu_j \cdot \theta_j + \kappa + \pi\sum_{j=1}^{i}\mu_j \quad (1 \le i \le N) \qquad (132)$$

The panel length is l_i and the panel inclination is δ_i of the *i*-th

panel, respectively.

We have to find proper angle $\theta_j \left(1 \le j \le N\right)$ on the unit circle so that the panel length l_i becomes exactly the same value as that of the given airfoil. Therefore for a given airfoil, the governing equation of the Schwartz-Christoffel panel method becomes

$$K \cdot 2^2 \cdot \int_{\theta_i}^{\theta_{i+1}} \prod_{j=1}^{N} \left|\sin \frac{\theta_j - \theta}{2}\right|^{\mu_j} \cdot d\theta = l_i \quad \left(1 \le i \le N\right). \quad (133)$$

The initial angle θ_1 on the unit circle can be chosen arbitrary and we can set $\theta_1 = 0$. We have $N-1$ unknown angles $\theta_j \left(2 \le j \le N\right)$. Also we have to determine extra two unknowns, i.e., the real constant K and κ. Therefore we have $N-1+2 = N+1$ unknowns altogether, although we have only N equations. The final equation is a requirement that a polygon must be closed one and given by

$$\sum_{j=1}^{N} \mu_j e^{i\theta_j} \left(= \sum_{j=1}^{N} \mu_j \cos \theta_j + i \cdot \sum_{j=1}^{N} \mu_j \sin \theta_j\right) = 0. \quad (134)$$

In the original version, we used this equation [2]. But during the course of the development, it was found that this equation could be replaced by

$$\sum_{i=1}^{N} l_i = P. \quad (135)$$

where P is the perimeter of the given airfoil approximated by N panels and it is a constant.

The governing equations are non-linear and the iteration is necessary to determine $\theta_i \left(2 \le i \le N\right)$, K and κ.

A possible solution procedure is as follows. A given airfoil chord locates on the ξ-axis $\left(0 \le \xi / c \le 1\right)$. The initial guess for $\theta_i \left(2 \le i \le N\right)$ may be given on the unit circle as follows.

$$\theta_i = \frac{2\pi}{N} \cdot (i-1) \quad \left(2 \le i \le N\right). \quad (136)$$

The first panel $(i=1)$ inclination measured counterclockwise from the ξ axis is $\delta = \delta_1$ and the geometrical condition becomes

$$\tan\left(\pi - \delta_1\right) = \frac{\eta_2 - \eta_1}{\xi_1 - \xi_2}. \quad (137)$$

where the right-hand side is caluculated from the given airfoil panel coordinate and

$$\delta_1 = \pi - \tan^{-1} \frac{\eta_2 - \eta_1}{\xi_1 - \xi_2}. \quad (138)$$

From Eq. (132) for the panel i, δ_1 satisfies

$$\delta_1 \equiv \frac{3}{2}\pi + \frac{1}{2}\sum_{j=1}^{N} \cdot \mu_j \cdot \theta_j + \kappa + \pi\mu_1. \quad (139)$$

From Eqs, (138) and (139), we can determine κ as follows.

$$\kappa = \delta_1 - \left[\frac{3}{2}\pi + \pi\mu_1 + \frac{1}{2}\sum_{j=1}^{N} \cdot \mu_j \cdot \theta_j\right]. \quad (140)$$

Once κ is determined, each panel inclination $\delta_i \left(2 \le i \le N\right)$ is also obtained.

We can evaluate each tentative panel length l_i' relative to K from Eq. (133) although we do not know the specific value of the real constant K at this stage.

$$\frac{l_i'}{K} = 2^2 \cdot \int_{\theta_i}^{\theta_{i+1}} \prod_{j=1}^{N} \left|\sin \frac{\theta_j - \theta}{2}\right|^{\mu_j} \cdot d\theta$$

$$\left[\equiv I\left(\theta_i, \theta_{i+1}\right)\right] \quad \left(1 \le i \le N\right) \quad (141)$$

The right-hand side of the above equation is a constant expressed by $I\left(\theta_i, \theta_{i+1}\right)$.

For the given airfoil, the exact total panel length, i.e. the perimeter is given by

$$P \equiv \sum_{j=1}^{N} l_j. \quad (142)$$

On the other hand, the perimeter during the iteration is given by

$$P' = \sum_{j=1}^{N} l_j' = K\sum_{j=1}^{N} I\left(\theta_j, \theta_{j+1}\right) = K \cdot I(0, 2\pi). \quad (143)$$

The geometric requirement is $P' = P$ and therefore K is determined as follows.

$$K = \frac{P}{I(0, 2\pi)}. \quad (144)$$

The above procedure is the first iteration (see Fig.11).

We then update the angles $\theta_i \left(2 \le i \le N\right)$. A simple update method can be as follows.

$$\theta_i^{new} = \theta_i - k \cdot \frac{\left(\sum_{j=1}^{i-1} l_j' - \sum_{j=1}^{i-1} l_j\right)}{\sum_{j=1}^{i-1} l_j} \quad (145)$$

$$\equiv \theta_i - k \cdot \left(\frac{\Delta s}{s}\right)_i \quad \left(2 \le i \le N\right)$$

where k is a positive constant and may be determined empirically. The above equation means that when the sum of the panel length up to i-th panel during the iteration $\sum_{j=1}^{i-1} l_j' \left(\equiv s_i'\right)$ exceeds that of the panel length $\sum_{j=1}^{i-1} l_j \left(\equiv s_i\right)$, the corresponding θ_i is reduced and vice versa. Convergence is reached when
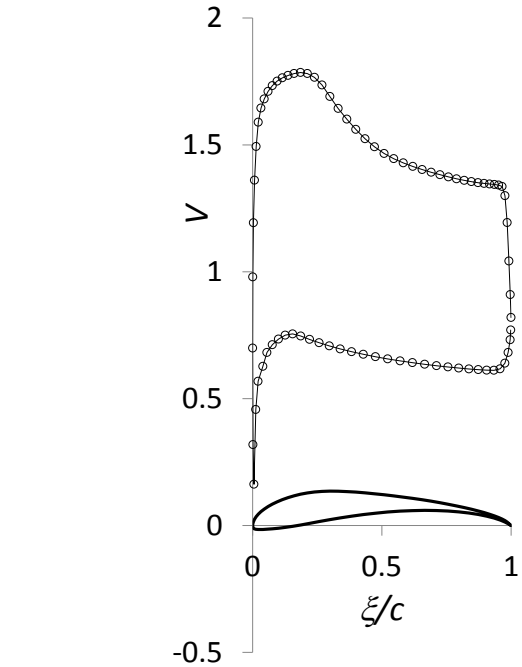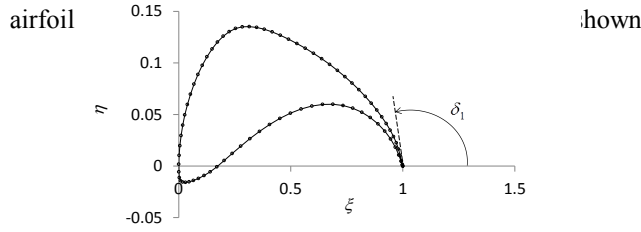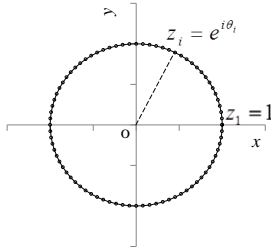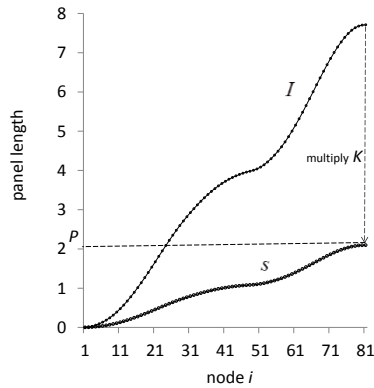
airfoil
hown

in Fig.12.

[1] airfoil N panels given

[2] assume $\theta_i = \dfrac{2\pi}{N} \cdot (i-1)$ $(2 \le i \le N)$, determine κ from δ_1

[3] K determined from integral I from airfoil perimeter P

$\theta_i^{new} = \theta_i - C \cdot \left(\dfrac{\Delta s}{s}\right)_i$

[4] update $\theta_i (2 \le i \le N)$ from excess panel length $(\Delta s/s)_i$ and obtain new κ

[5] repeat [3] and [4] to achieve $\left|\Delta s/s\right|_i < \varepsilon$ and restore original airfoil

Fig. 11. Schwartz-Christoffel panel method iteration procedure

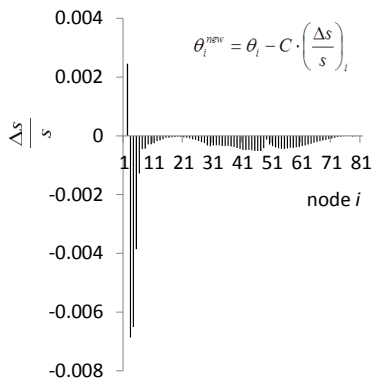Fig.12. S1223 airfoil surface $|V|$ at $C_l \approx 1.95$ (cf. [8])

$$\frac{|l_i' - l_i|}{l_i} < \varepsilon . \qquad (146)$$

where ε is a small positive constant $(\varepsilon \ll 1)$ and we finally determine $\theta_i (2 \le i \le N)$, K and κ .

The panel surface velocity is given by

$$\left(\frac{dw}{d\zeta}\right)\Big|_i = \frac{\sin(\theta_{i\,\mathrm{mid}} - \alpha_z) + \sin\alpha_z}{2 \cdot \prod\limits_{j=1}^{N}\left|\sin\dfrac{\theta_j - \theta_{i\,\mathrm{mid}}}{2}\right|^{\mu_j}} \cdot e^{-i\beta_i} . \qquad (147)$$

where

$$\theta_{i\,\mathrm{mid}} \equiv \frac{\theta_i + \theta_{i+1}}{2} . \qquad (148)$$

$$\beta_i = -\pi\mu_1 - \pi + \delta_1 + \pi\sum_{j=1}^{i}\mu_j . \qquad (149)$$

and

$$C_l = 4 \cdot \left(\frac{K}{c}\right) \cdot 2\pi\sin\alpha_z . \qquad (150)$$

The average velocity along the i-th panel can be calculated as follows.

$$\begin{aligned}
\frac{dw}{d\zeta} \cdot d\zeta &= (u - iv) \cdot (d\xi + id\eta) \\
&= u \cdot d\xi + v \cdot d\eta + i(ud\eta - vd\xi) \cdot \\
&= \mathrm{V} \cdot d\mathrm{l} = Vdl
\end{aligned} \qquad (151)$$

When we integrate counterclockwise along the panel surface, we get

$$-\overline{V} \cdot l = -\int_{\theta_i}^{\theta_{i+1}} Vdl = -V_\infty \int_{\theta_i}^{\theta_{i+1}} \frac{dw}{d\zeta} \cdot d\zeta$$

$$= -2KV_\infty \left[\cos(\theta - \alpha_z) - \theta \cdot \sin\alpha_z\right]_{\theta_i}^{\theta_{i+1}}$$

Therefore the average velocity along the each panel i becomes

$$\frac{\overline{V}_i}{V_\infty} = -\frac{K}{l_i} \cdot 2 \cdot \begin{bmatrix} \cos(\theta_{i+1} - \alpha_z) - \cos(\theta_i - \alpha_z) \\ -(\theta_{i+1} - \theta_i) \cdot \sin\alpha_z \end{bmatrix}. \quad (152)$$

The moment around the leading edge can be derived as follows.

$$dC_M = -C_p \eta d\eta - C_p \xi d\xi = \left[\left(\frac{V}{V_\infty}\right)^2 - 1\right](\xi d\xi + \eta d\eta). \quad (153)$$

When the panel average velocity is used, the moment becomes (excluding -1 term)

$$dC_M \approx \left(\frac{\overline{V}}{V_\infty}\right)^2 (\xi d\xi + \eta d\eta) = \left(\frac{\overline{V}}{V_\infty}\right)^2 \frac{1}{2} d(\xi^2 + \eta^2). \quad (154)$$

So the panel moment contribution can be approximated as follows.

$$\Delta C_{M_i} \approx \frac{1}{2}\left(\frac{\overline{V}}{V_\infty}\right)^2 \left[|\zeta_{i+1}|^2 - |\zeta_i|^2\right]. \quad (155)$$

Note that the present method can analyze airfoils with very sharp leading and/or trailing edges, e.g. Joukowski airfoil [9] and Gurney flap [10]. The conventional panel methods generally suffer to solve these problems [11],[12].

VI. Concluding Remarks

We apply the Schwartz-Christoffel transformation to regular polygons and airfoils.

For the regular polygons, the Schwartz-Christoffel transformation is expressed in a concise simple form and the aerodynamic characteristics are obtained semi-analytically. For a regular polygon with even sides $n = 2m(m = 1,2,3,...)$, the maximum velocity at its own shoulder surface is expressed as $2^{[(m-1)/m]}$ relative to the incoming uniform flow.

Triangular, diamond and hexagonal airfoils are also analyzed. A rudder analytical solution is repeated here to show the usefulness of the transformation.

A given airfoil section is also calculated. An improved numerical solution procedure is shown.

In spite of the numerical nature of the present method, lift is expressed in a closed analytical form. Moment is also obtained numerically (and semi-analytically) based on the analytical average of the velocity on the each panel.

References

[1] B.K. Shivamoggi, *Theoretical Fluid Dynamics*, John Wiley & Sons, 1998, p.53.

[2] R. Fukatsu,"Aerofoil Theory with Flap (in Japanese)", Imperial U Tokyo Aeronaut. Lab. Rep., no. 55, pp.47-64, Mar.1929.

[3] E. Morishita, E., "Schwartz-Christoffel Panel Method", Trans.JSASS, vol.47, no. 156, pp.153-157, Aug. 2004.

[4] T. Moriya, *Introduction to Aerodynamics* (in Japanese), Baifu-kan, 1977, p.139.

[5] I. Imai, *Fluid Dynamics and Complex Analysis* (in Japanese), Nihon Hyoron-sha, Tokyo, 1981, pp.174—175

[6] Z.W. Tian & Z.N. Wu, "A Study of Two-Dimensional Flow past Regular Polygons via Conformal Mapping", J. Fluid Mech., vol. 628, pp.121-154, 2009.

[7] K. Yonezawa., Y. Goto, S. Sunada, T. Hayashida, T. Suwa, N. Sakai,, H. Nagai, K. Asai, & Y. Tsujimoto,"An Investigation of Airfoils for Development of a Propeller of Mars Exploration Airplane(in Japanese)", J. JSASS, vol. 62, no. 1, pp.24-30, Feb. 2014.

[8] M.S. Selig, & J.J. Guglielmo,"High-Lift Low Reynolds Number Airfoil Design", J Aircraft, vol. 34, no. 1, pp.72-79, Jan.-Feb. 1997.

[9] R.L. Panton, *Incompressible Flow*, John Wiley & Sons, 2013, p.475,

[10] Y. Li, J. Wang & P. Zhang," Effects of Gurney Flap on a NACA0012 Airfoil," Flow Turbulence and Combustion, vol. 68, no.1, pp.27-39, Jan. 2002.

[11] J. Moran, J, *An Introduction to Theoretical and Computational Aerodynamics*, John Wiley & Sons , 1984, p.286.

[12] S. Tanaka, S. Murata & K. Kurata, "Computation of the Potential Flow through Cascades using the Conformal Mapping and the Singularity Method", JSME International Journal, Series II, vol. 34, no. 2, pp.423-430, Nov. 1991.